Reaction mechanism for $^{12}C(e,e'n)^{11}C$ in the continuum above the giant resonance

K. Takahisa,* T. Saito,† S. Suzuki,‡ C. Takakuwa,§ and M. Oikawa‖
Laboratory of Nuclear Science, Tohoku University, Mikamine, Taihaku-ku, Sendai 982-0826, Japan

T. Nakagawa¶ and T. Tohei¶
Department of Physics, Tohoku University, Aramaki, Aoba-ku, Sendai 980-8578, Japan

K. Abe
Department of Nuclear Engineering, Tohoku University, Aramaki, Aoba-ku, Sendai 980-8579, Japan
(Received 14 January 2002; published 16 July 2002)

Out-of-plane measurements of the angular correlations for the $^{12}C(e,e'n)^{11}C$ reaction have been performed in the continuum above the giant resonance. The cross sections were directly separated into the longitudinal and transverse, longitudinal-transverse, and transverse-transverse components. Recent random-phase approximation (RPA) predictions reproduce fairly well the angular correlations of both the $^{12}C(e,e'n_{0,1})$ and $^{12}C(e,e'p_0)$ reactions, but the Hartree-Fock predictions fail to reproduce that of $(e,e'n_{0,1})$. It suggests that RPA correlations are crucial for the interpretation of the $(e,e'n_{0,1})$ reaction in the observed excitation energy region.

DOI: 10.1103/PhysRevC.66.014605 PACS number(s): 25.30.Fj, 23.20.−g, 24.30.−v, 27.20.+n

The reaction mechanisms for the photon- or electron-nucleon emission reaction have been studied extensively. Most studies have been done in the giant dipole resonance (GDR) region, where the reaction mechanism is quite well understood. In the continuum above the GDR, experimental data are rather scarce and the reaction mechanism is not yet clear.

Recently, Ryckebusch *et al.* [1] have performed a self-consistent random-phase approximation (RPA) calculation with a Skyrme-type effective interaction for the $^{16}O(\gamma,N)$ cross sections and angular distributions with a decomposition into three different dynamical effects: First, the contribution from a direct reaction mechanism, which is calculated by using the one-body current. Second, the contribution of the exchange current in the direct reaction matrix element. Third, the contribution coming from a coupling of the initial and final states to the giant resonance (correlation). The calculated angular distributions for the $^{16}O(\gamma,p_0)$ and $^{16}O(\gamma,n_0)$ reactions at $E_\gamma = 23$ and 80 MeV indicate that the reaction mechanism changes completely with increasing photon energies. In the giant resonance region the main contribution to the cross section comes from correlation effects, the direct reaction mechanism contribution being small. On the other hand, the RPA calculations at 80 MeV reveal that the (γ,p_0) and (γ,n_0) cross sections are of the same order of magnitude, but the reaction mechanism is quite different; the direct contribution constitutes an important part of the p_0 angular contribution and determines essentially the form of it, but in the n_0 one the correlation effects are dominant and the direct contribution is negligible.

Based on the above calculations for the photoreaction, it is important to compare the $(e,e'p)$ and $(e,e'n)$ reactions in order to understand the reaction mechanism for $(e,e'n)$. Out-of-plane measurements of protons from the $^{12}C(e,e'p)$ reaction have recently been carried out at an energy transfer of 40 MeV and momentum transfer of 0.35 fm^{-1}. The longitudinal-transverse interference term, as well as the non-interference term of the $(e,e'p_0)$ angular correlation has been obtained [2]. The angular correlations were well reproduced by the RPA calculations [3]. A few studies for the $(e,e'n)$ reaction in the giant resonance region have been performed [4], but there are no measurements in the continuum above the giant resonance. The reaction mechanism of the $(e,e'n)$ reaction in the continuum has not yet been clarified. It is to be expected that in this reaction the quasi-free knockout (QFK) process is very small in contrast to the $(e,e'p)$ reaction. In previous papers on the $^{12}C(e,e'n)$ experiments including out-of-plane measurements [5,6], we reported that the cross section at the peak of the GDR was found to be almost totally longitudinal, and its angular correlation indicated a strong forward-backward asymmetry that was reproduced by the multipole expansion with $E0$ and $E2$ components in addition to $E1$. The present paper reports on out-of-plane measurements of the angular correlations of the $^{12}C(e,e'n_{0,1})$ reaction in the continuum above the giant resonance, and compares the results with those of the $^{12}C(e,e'p_0)$ reaction and the RPA predictions. Preliminary results have been presented in Ref. [7].

*Present address: Research Center for Nuclear Physics, Osaka University, Ibaraki 567-0047, Japan.

†Present address: Faculty of Engineering, Tohoku Gakuin University, Chuo, Tagajo 985-8537, Japan.

‡Present address: Japan Synchrotron Radiation Research Institute, Mikazuki-cho, Sayogun, Hyogo 679-5198, Japan.

§Present address: Research & Development Center, Toshiba Co. Shinsugita-cho, Isogo-ku, Yokohama 235-8522, Japan.

‖Present address: 5th Research Center, Technical Research & Development Institute, Japan Defense Agency, Nagase, Yokosuka 239-0826, Japan.

¶Present address: Tohoku Institute of Technology, Kasumi-cho, Taihaku-ku, Sendai 982-8577, Japan.

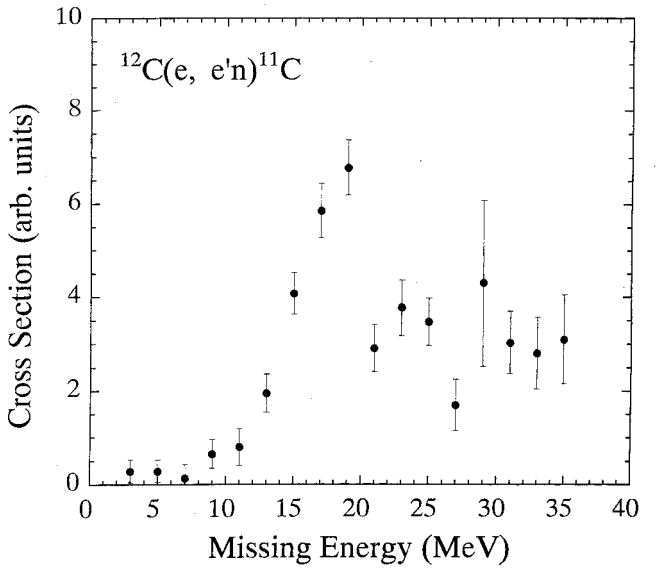

FIG. 1. Missing energy spectrum for the $^{12}C(e,e'n)^{11}C$ reaction at 45 MeV.

The experiment was performed using the continuous electron beam from the 150-MeV Tohoku University pulse stretcher ring [8]. A natural carbon target of thickness 105 mg/cm^2 was bombarded with electrons of energy 129 MeV. The scattered electrons were detected at $\theta_e=30°$ by a magnetic spectrometer that has a solid angle of 5 msr and a momentum resolution of 0.05% within an accepted momentum bite of 5.3%. The emitted neutrons were detected using ten NE213 liquid scintillator neutron detectors.

Six detectors were placed in the electron scattering plane ($\phi=180°$) at $\theta_n=0°$, 30°, 60°, 90°, 180°, and 210°, three detectors were placed out of the scattering plane ($\phi=135°$) at $\theta_n=30°$, 60°, 90°, and one detector was placed out of plane ($\phi=90°$) at $\theta_n=30°$, where θ_n is measured from the momentum-transfer vector. Each detector was placed 1.0 m from the center of the scattering chamber allowing the neutron energy to be determined by a time-of-flight method. The neutron detectors were shielded with lead, paraffin, and concrete, and lead collimators were placed in front of 4-cm-thick bismuth plates to absorb scattered electrons and soft γ rays from the target. The neutron detectors were calibrated using γ rays from ^{22}Na, ^{137}Cs, ^{60}Co, and Am-Be sources. The Compton edge of the ^{88}Y γ ray (1.61 MeV) was utilized to set the detection threshold. The neutron efficiency for the detectors was determined using a ^{252}Cf source and a Monte Carlo code. The details of electronics, data acquisition, and detection efficiency are described elsewhere [9].

The angular correlations and cross sections have been measured mainly at 45 MeV and less accurately at excitation energies of 30–55 MeV. The missing energy spectrum for the $^{12}C(e,e'n)^{11}C$ reaction is shown in Fig. 1. The peak at 19 MeV corresponds to the ground state transition of 18.7 MeV. But as the energy resolution is not adequate, we regard this peak as the yield from population of both the ground and first-excited states. The angular correlation at 45 MeV is shown in Fig. 2. The in-plane angular correlation indicates a

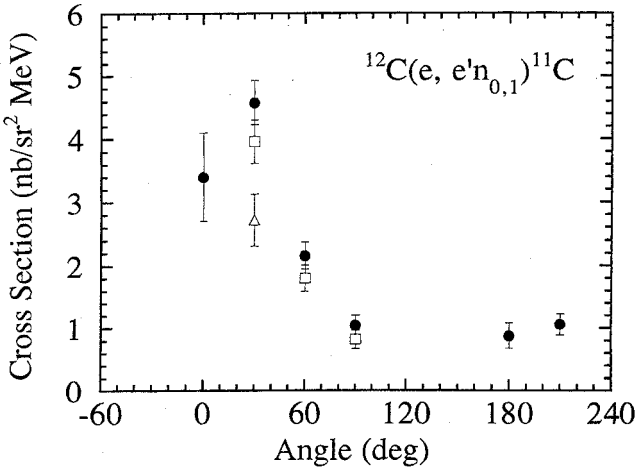

FIG. 2. Angular correlations for the $^{12}C(e,e'n_{0,1})^{11}C$ reaction at $\theta_e=30°$, $\epsilon_i=129$ MeV, and $\omega=45$ MeV. The solid circles, open squares, and open triangles represent in-plane ($\phi=180°$), out-of-plane ($\phi=135°$), and out-of-plane ($\phi=90°$) measurements, respectively.

sharper forward peak asymmetry than that of the giant resonance in ^{12}C [5,6]. A large difference was observed between the cross sections at $\phi=180°$ and $\phi=90°$, which indicates the existence of a longitudinal-transverse interference component.

Separation of the interference and noninterference terms has been done by the following method. If we represent the noninterference, longitudinal-transverse, and transverse-transverse components with *A*, *B*, and *C*, respectively, the cross section can be written as

$$\sigma(\phi)=A+B\cos\phi+C\cos 2\phi. \quad (1)$$

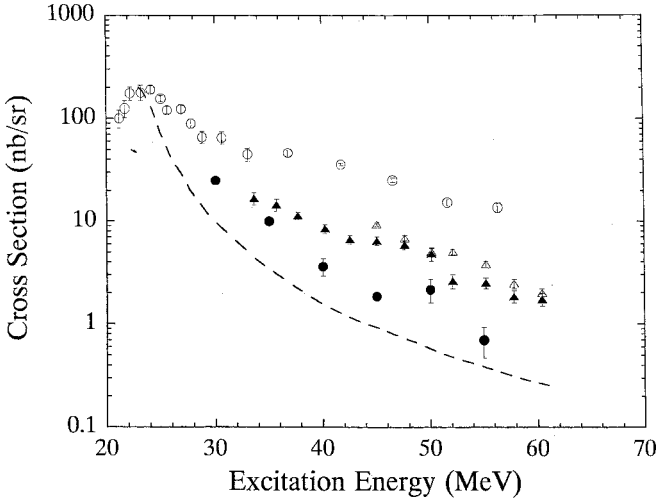

FIG. 3. Comparison of the $^{12}C(e,e'n_{0,1})^{11}C$ cross section with cross sections for other reactions. Symbols are as follows: ● for $(e,e'n_{0,1})$; ○ for $(e,e'p_{0,1})$ Ref. [10]; ▲ for $(\gamma,n_{0,1})$ Ref. [12]; and △ for $(\gamma,p_{0,1})$ Ref. [13]. Dashed line is a Lorentz shape normalized to the $^{12}C(\gamma,n)$ cross section of Ref. [14] at the peak of the GDR.

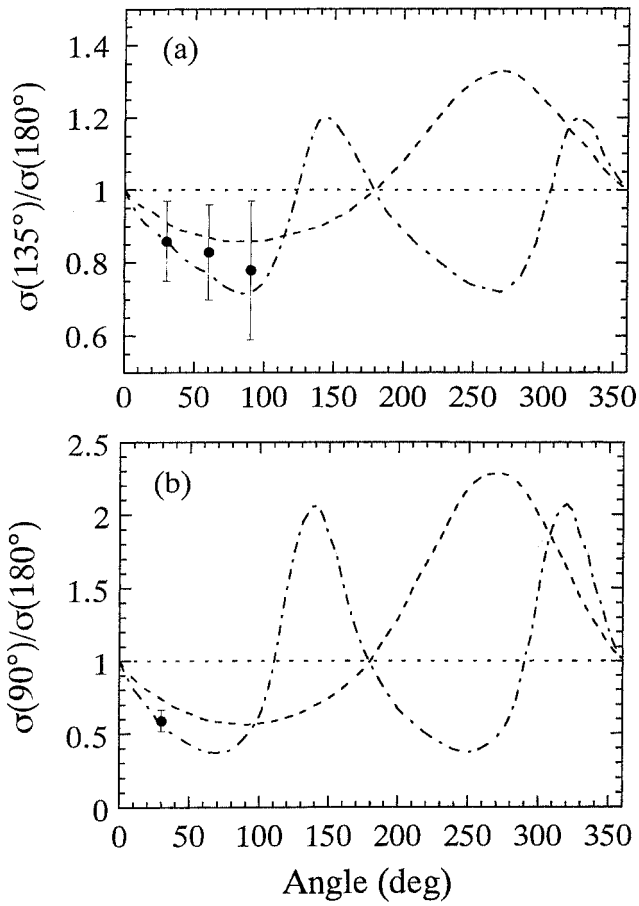

FIG. 4. Ratio of out-of-plane to in-plane cross sections at 45 MeV as a function of scattering angle for the $^{12}C(e,e'n_{0,1})^{11}C$ reaction. The dashed, dot, and dot-dashed lines are calculations for the CEP, QFK and GDR, respectively.

From the measurements at $\phi=180°$, 135°, and 90°, *A*, *B*, and *C* are obtained as

$$A=[\sigma(180°)-\sqrt{2}\sigma(135°)+\sigma(90°)]/(2-\sqrt{2}),$$

$$B=[\sigma(180°)-2\sigma(135°)+\sigma(90°)]/(\sqrt{2}-1), \qquad (2)$$

$$C=[\sigma(180°)-\sqrt{2}\sigma(135°)+(\sqrt{2}-1)\sigma(90°)]/(2-\sqrt{2}).$$

Using the cross sections at $\theta_n=30°$ in Fig. 2, the noninterference, longitudinal-transverse, and transverse-transverse components were obtained as 2.9 ± 1.2, -1.5 ± 2.1, and 0.2 ± 1.6 nb/sr^2 MeV, respectively. Compared the corresponding values of 26.4 ± 6.1, 0.1 ± 10.5, and -1.3 ± 5.3 nb/sr^2 MeV measured in the giant resonance [6], the noninterference component decreases by about one order of magnitude.

Figure 3 shows the excitation energy dependence of the $^{12}C(e,e'n_{0,1})$ cross section compared with other reaction cross sections. The $^{12}C(e,e'n_{0,1})$ cross sections were obtained from each angular correlation measured at excitation energies of 35, 40, 45, 50, and 55 MeV. The $^{12}C(e,e'p_{0,1})$ cross sections measured at $\epsilon_i=122$ MeV and $\theta_e=56°$ [10] have been transformed into those at the present momentum transfer using the Goldhaber-Teller model [11] under an assumption of $E1$ excitation, which is larger than the $(e,e'n_{0,1})$ cross section by one order of magnitude. The transformed $^{12}C(\gamma,n_{0,1})$ [12] and $^{12}C(\gamma,p_{0,1})$ [13] cross sections agree well, but they are larger than the $(e,e'n_{0,1})$ cross section in the excitation energy range of 40–55 MeV. The dashed line indicates a Lorentz shape that is normalized to the $^{12}C(\gamma,n)$ cross section [14] at the peak of the GDR. Each cross section of the $(e,e'n_{0,1})$, $(e,e'p_{0,1})$, $(\gamma,n_{0,1})$, and $(\gamma,p_{0,1})$ reactions at 45 MeV is larger than the tail of the GDR. This suggests that there might be reaction mechanisms besides the GDR (correlation).

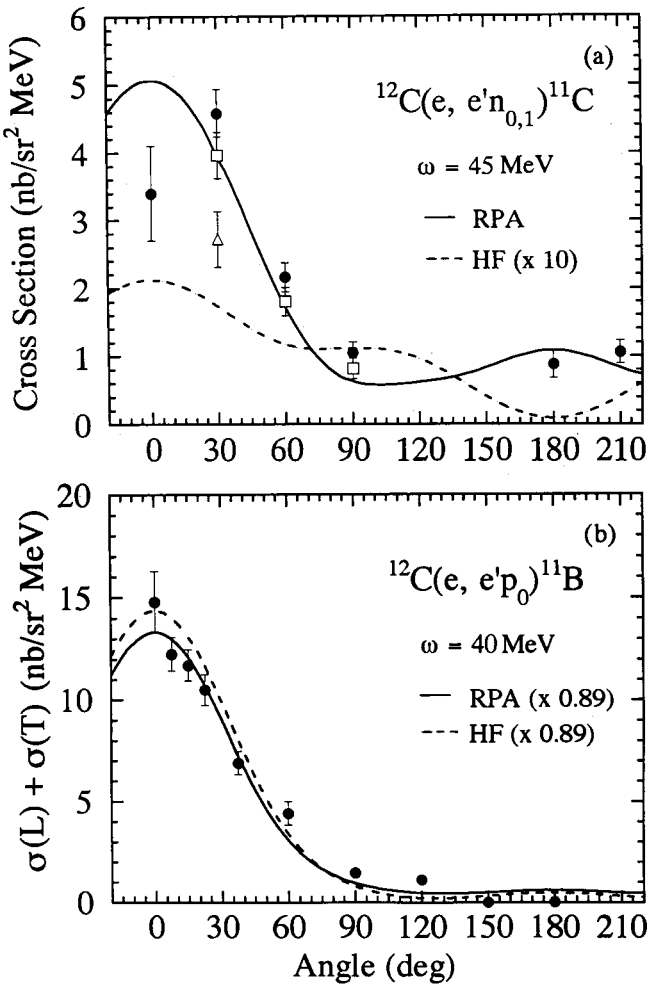

FIG. 5. Comparison of the $^{12}C(e,e'n_{0,1})^{11}C$ and $^{12}C(e,e'p_0)^{11}B$ (Ref. [2]) angular correlations with the HF (dashed line) and RPA (solid line) predictions [2,3]. The cross section for $(e,e'p_0)$ is that for the noninterference component. The calculations have been performed for $\omega=40$ MeV at $\epsilon_i=129$ MeV and $\theta_e=30°$. The calculated values of HF for $(e,e'n_{0,1})$ are scaled up by a factor of 10. Those for both HF and RPA for $(e,e'p_0)$ are scaled down by a factor of 0.89.

In Fig. 4 the out-of-plane data are compared with simple calculations based on the assumptions of three types of the reactions: the GDR, QFK, and charge exchange process (CEP). For the GDR, the coincidence cross section given by Kleppinger and Walecka [15] was used. The cross section for the QFK process was deduced from the equation for the el-

ementary electron-nucleon interaction in the nucleus in the plane wave impulse approximation (PWIA) [16]. In this expression, the cross section has no longitudinal-transverse and transverse-transverse terms since there are no contributions stemming from the convection current and the charge density operators. Thus the angular correlation has no ϕ dependence. In the CEP, the shape of the angular correlation was assumed to be the same as those for the $^{12}C(e,e'p_0)^{11}B$ reaction calculated in the PWIA [16]. The cross section ratios of $\sigma(\phi_n=135°)/\sigma(\phi_n=180°)$ are compared with three kinds of the calculations in Fig. 4(a). From the figure, experimental data differ from the QFK prediction, but it is not able to distinguish between the GDR and CEP as a favorable mechanism within the experimental error. In Fig. 4(b) the cross section ratio $\sigma(\phi_n=90°)/\sigma(\phi_n=180°)$ is compared with three kinds of the calculations similar to Fig. 4(a). It seems that the GDR mechanism is consistent with the data. However, the $(e,e'n_{0,1})$ cross section at 45 MeV cannot be explained only in terms of the tail of the GDR cross section as shown in Fig. 3.

The angular correlation for the $^{12}C(e,e'n_{0,1})$ reaction is compared with that for the $^{12}C(e,e'p_0)$ reaction and the predictions in Fig. 5. The cross section for $(e,e'p_0)$ in the figure is that for the noninterference component. Both the angular correlations show a sharp forward peak, but the backward component is less for $(e,e'p_0)$. Hartree-Fock (HF) and RPA calculations have been performed by Ryckebusch [2,3] for both the $^{12}C(e,e'n_0)$ and $^{12}C(e,e'p_0)$ reactions, for an excitation energy of $\omega=40$ MeV at an incident energy of $\epsilon_i=129$ MeV and a scattering angle of $\theta_e=30°$. The HF approach corresponds to a QFK reaction mechanism and its predictions are uniquely determined by the single-particle properties of the target nucleus. On the other hand, the contribution from initial and final state correlations is accounted for through the RPA. In the RPA calculation, the mean-field parameters are determined through a HF procedure with a *SkE2* effective interaction [3]. All natural and unnatural parity strengths up to $J=5$ are included in the calculation. The spectroscopic factor for the $^{12}C(e,e'p_0)$ transition is taken to be 1.82, which was obtained from the quasielastic $(e,e'p_0)$ experiment performed at NIKHEF [17]. In the $(e,e'n_{0,1})$ calculations the same parameters as those for $(e,e'p_0)$ are used except for the total $1p$ spectroscopic factor of 2.23. Figure 5(a) shows a comparison of the $^{12}C(e,e'n_{0,1})$ angular correlation with the predictions. The HF prediction is one order of magnitude smaller than the RPA prediction. The RPA prediction reproduces the experimental angular correlations well, including backward components. On the other hand, in the $(e,e'p_0)$ reaction the HF and RPA predictions are almost identical as shown in Fig. 5(b). These predictions reproduce the experimental angular correlations well although the calculated values are scaled down by 0.89. The RPA predictions reproduce the angular correlations of both the $^{12}C(e,e'n_{0,1})$ and $^{12}C(e,e'p_0)$ reactions fairly well, but the HF predictions fail to reproduce that of $(e,e'n_{0,1})$. It suggests that long-range correlations of the RPA type and multistep processes which it induces are crucial for the $(e,e'n_{0,1})$ reaction in the continuum above the giant resonance. This result is consistent with the calculated angular distribution at 80 MeV for the $^{16}O(\gamma,p_0)$ and $^{16}O(\gamma,n_0)$ reactions [1].

In summary, we have performed out-of-plane measurements of the angular correlations for the $^{12}C(e,e'n)^{11}C$ reaction in the continuum above the giant resonance at a momentum transfer of 0.35 fm^{-1}. The angular correlations were separated into the longitudinal and transverse, longitudinal-transverse, and transverse-transverse components. The ratios of the longitudinal-transverse and transverse-transverse to the noninterference component suggest that the GDR and/or the CEP play a role in the reaction mechanism for the $^{12}C(e,e'n_{0,1})^{11}C$ reaction. Both the $(e,e'n_{0,1})$ and $(e,e'p_0)$ angular correlations were compared with recent HF and RPA predictions. The RPA predictions reproduce the angular correlations of both the $^{12}C(e,e'n_{0,1})$ and $^{12}C(e,e'p_0)$ reactions fairly well, but the HF predictions fail to reproduce that of $(e,e'n_{0,1})$. This suggests that RPA correlations are crucial for the interpretation of the $(e,e'n_{0,1})$ reaction. This result is consistent with the observations made from the calculated angular distributions for the photoreaction.

We wish to thank J. Ryckebusch for providing us with calculations and helpful comments. We are grateful to M. N. Thompson for the careful reading of the manuscript and discussions. We would like to thank the linac crew of the Laboratory of Nuclear Science for providing the quality beam.

[1] J. Ryckebusch *et al.*, Nucl. Phys. **A476**, 237 (1988).
[2] T. Tadokoro *et al.*, Nucl. Phys. **A575**, 333 (1994).
[3] J. Ryckebusch *et al.*, Nucl. Phys. **A503**, 694 (1989).
[4] K. Kino *et al.*, Phys. Rev. C **65**, 024604 (2002), and references therein.
[5] T. Saito *et al.*, Phys. Rev. Lett. **78**, 1018 (1997).
[6] M. Oikawa *et al.*, Phys. Rev. Lett. **84**, 2338 (2000).
[7] T. Saito *et al.*, in *Proceedings of the Fourth International Spring Seminar on Nuclear Physics, Amalfi, Italy, 1992*, edited by A. Covello (World Scientific, Singapore, 1993), p. 401.
[8] T. Tamae *et al.*, Nucl. Instrum. Methods Phys. Res. A **264**, 173 (1988).
[9] S. Suzuki *et al.*, Nucl. Instrum. Methods Phys. Res. A **314**, 547 (1992).
[10] B. B. Wojtsekhowski (private communication).
[11] M. Goldhaber and E. Teller, Phys. Rev. **74**, 1046 (1948).
[12] P. D. Harty *et al.*, Phys. Rev. C **37**, 13 (1988).
[13] K. Mori *et al.*, Phys. Rev. C **51**, 2611 (1995).
[14] S. C. Fultz *et al.*, Phys. Rev. **143**, 790 (1966).
[15] W. E. Kleppinger and J. D. Walecka, Ann. Phys. (N.Y.) **146**, 349 (1983).
[16] M. Cavinato *et al.*, Z. Phys. A **335**, 401 (1990).
[17] L. Lapikás, G. van der Steenhoven, L. Frankfurt, M. Strikman, and M. Zhalov, Phys. Rev. C **61**, 064325 (2000).